ChemComm

COMMUNICATION

Strong direct exchange coupling and single-molecule magnetism in indigo-bridged lanthanide dimers

Received 00th January 20xx,
Accepted 00th January 20xx

DOI: 10.1039/x0xx00000x

www.rsc.org/ChemComm

Fu-Sheng Guo[a] and Richard A. Layfield*[a]

The synthesis, structure and magnetic properties of the indigo-bridged dilanthanide complexes $[\{(\eta^5\text{-Cp}^*)_2\text{Ln}\}_2(\mu\text{-ind})]^{n-}$ with Ln = Gd or Dy and *n* = 0, 1 or 2 are described. The gadolinium complexes with *n* = 0 and 2 show typically weak exchange coupling, whereas the complex bridged by the radical $[\text{ind}]^{3-}$ ligand shows an unusually large coupling constant of $J = -11\ \text{cm}^{-1}$ ($-2J$ formalism). The dysprosium complexes with *n* = 0 and 1 are single-molecule magnets in zero applied field, whereas the complex with *n* = 2 does not show slow magnetic relaxation.

Naturally occurring indigo (H_2ind) and many of its synthetic derivatives have a well-established history in the dyes and pigments industry, and they have recently attracted attention owing to their applications in organic electronics, particularly as field-effect transistors (OFETs).[1] Another property of indigo that has until recently received surprisingly little attention is its ability to serve as a chelate ligand in the doubly deprotonated form, i.e. $[\text{ind}]^{2-}$. The presence of two binding pockets within the indigo framework lends itself to the formation of binuclear complexes and supramolecular architectures,[2] and the π-orbital structure of the ligand is of interest owing to the range of additional oxidation levels that become accessible upon complexation.[3] Radical forms of indigo ligands are particularly intriguing targets owing to their potential for enabling electronic communication between metal centres in binuclear complexes, however very few examples are known, all of which focus on a limited selection of 4d and 5d transition metals.[4]

We now describe the synthesis, structures and magnetic properties of the first lanthanide complexes of indigo ligands, i.e. the bimetallic complexes $[\{(\eta^5\text{-Cp}^*)_2\text{Ln}\}_2(\mu\text{-ind})]^{n-}$ in which Ln = Gd or Dy, and *n* = 0, 1 or 2. The motivation for studying the gadolinium complexes stems from the magnetic exchange coupling, which should be significantly stronger in the $[\text{ind}]^{3-}$ radical-bridged species $[\{(\eta^5\text{-Cp}^*)_2\text{Gd}\}_2(\mu\text{-ind})]^{n-}$ than in the analogues containing the closed-shell ligands $[\text{ind}]^{2-}$ and $[\text{ind}]^{4-}$. For the dysprosium analogues, the single-molecule magnet (SMM) properties are of interest.[5] Metallocene-based SMMs containing the $[(\eta^5\text{-Cp}')_2\text{Dy}]^+$ building block (Cp' = various cyclopentadienyl ligands) were introduced by our group and subsequently developed by us and others:[6,7] in such SMMs, very large effective energy barriers to reversal of the magnetization (the anisotropy barrier, U_{eff}) are possible. A magneto-structural correlation was developed to explain the properties of these SMMs, in which the $[\text{Cp}']^-$ ligands create a strong axial potential that complements the oblate 4f electron density of the Dy^{3+} cation, with the magnitude of U_{eff} being moderated by the crystal field effects of the equatorial ligands. For example, in the pnictogen-bridged SMMs $[(\eta^5\text{-Cp}'_2\text{Dy})\{\mu\text{-E(H)Mes}\}]_3$ (E = P, As, Sb; Mes = mesityl), as the Dy–E bonds lengthen the value of U_{eff} increases from 200 cm^{-1} to 345 cm^{-1} in zero applied field.[6]

Although the magneto-structural correlation described above readily explains the properties of metallocene SMMs with soft equatorial donor ligands, analogous SMMs with hard equatorial donors, such as those provided by indigo ligands, have not yet been considered. Additional intrigue is provided by dysprosium metallocenes bridged by radical ligand such as $[\text{ind}]^{3-}$, and the evaluation of the magnetic properties of such a system is described herein.[8] Thus, the gadolinium and dysprosium compounds $[(\text{Cp}^*_2\text{Ln})_2(\mu\text{-ind})]$ (**1**$_{\text{Ln}}$), $[\text{K(thf)}_6][(\text{Cp}^*_2\text{Ln})_2(\mu\text{-ind})]\cdot\text{thf}$ ($[\text{K(thf)}_6][\mathbf{2}_{\text{Ln}}]\cdot\text{thf}$), and $[\{\text{K(thf)}_3\}_2\{\text{Cp}^*_2\text{Ln}\}_2(\mu\text{-ind})\}]$ ($[\{\text{K(thf)}_3\}_2(\mathbf{3}_{\text{Ln}})]$) were synthesized according to Scheme 1. Complexes **1**$_{\text{Ln}}$ were isolated in yields of 40-45% via the propene elimination reactions of $[\text{Cp}^*_2\text{Ln}(\text{C}_3\text{H}_5)]$[9] with indigo. Subsequently, one-electron reduction of **1**$_{\text{Ln}}$ with KC_8 produced the radical-bridged complexes $[\text{K(thf)}_6][\mathbf{2}_{\text{Ln}}]\cdot\text{thf}$ in yields of 25%, and two-electron reduction of **1**$_{\text{Ln}}$ with KC_8 produced $[\{\text{K(thf)}_3\}_2(\mathbf{3}_{\text{Ln}})]$ in yields of 55-60%.

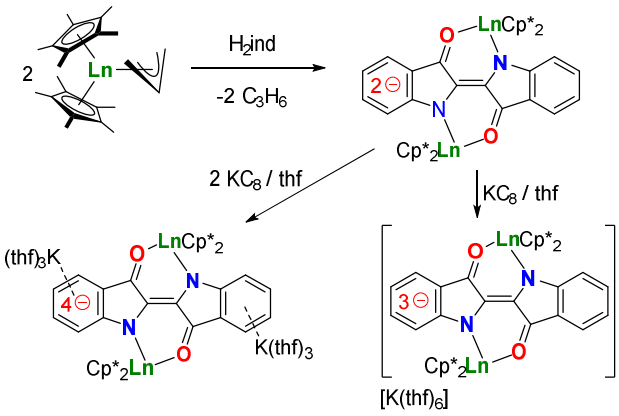

Scheme 1 Synthesis of **1**$_{\text{Ln}}$, $[\text{K(thf)}_6][\mathbf{2}_{\text{Ln}}]$ and $[\{\text{K(thf)}_3\}_2(\mathbf{3}_{\text{Ln}})]$ (Ln = Gd, Dy).

Single-crystal X-ray structural analysis of all six compounds (Table S1) revealed that the gadolinium versions of each compound are structurally very similar to their dysprosium-containing analogues. Complexes $\mathbf{1_{Ln}}$ (Figs 1, S7) are non-centrosymmetric dimers consisting of two lanthanide ions, each of which is complexed by an *N*,*O*-bound $[ind]^{2-}$ ligand and two η^5-Cp* ligands. Each metal is formally eight-coordinate and resides in a distorted C_s-symmetric environment. The structures of $[K(thf)_6][\mathbf{2_{Ln}}]$ consist of the centrosymmetric complex anions $[\{(\eta^5\text{-Cp*})_2Ln\}_2(\mu\text{-ind})]^-$ ($\mathbf{2_{Ln}}$, Figs 1, S8) and an ion-separated $[K(thf)_6]^+$ cation. In contrast, $[\{K(thf)_3\}_2(\mathbf{3_{Ln}})]$ are ion-contacted species, in which centrosymmetric $[\{(\eta^5\text{-Cp*})_2Ln\}_2(\mu\text{-ind})]^{2-}$ complexes ($\mathbf{3_{Ln}}$, Figs 1, S9) coordinate to two $[[K(thf)_3]^+$ cations via cation-π interactions between potassium and the aromatic rings of the indigo ligand. Beyond the qualitative similarities, analysis of the bond lengths and angles in $\mathbf{1_{Dy}}$, $\mathbf{2_{Dy}}$ and $\mathbf{3_{Dy}}$ reveals that the one-electron and two-electrons reduction processes produce minor structural changes in the coordination environment of the dysprosium centres and in the indigo ligand. Upon reduction, the Dy–N bond lengths decrease by 0.048 Å from 2.383(3)/2.391(3) Å in $\mathbf{1_{Dy}}$ to 2.343(4) Å in $\mathbf{2_{Dy}}$, before increasing slightly to 2.352(3) Å upon reduction to $\mathbf{3_{Dy}}$. The Dy–O bond lengths vary in a similar manner, resulting in slight increases in the N-Dy-O angle from 78.4(1)° to 81.8(1)° to 83.2(1)°. The length of the central carbon-carbon bond linking the two halves of the indigo ligands (C_c-C_c in Table 1) increases slightly from 1.391(6) Å to 1.423(4) Å and to 1.452(7) Å as the formal charge on the ligand increases from –2 to –3 to –4 in $\mathbf{1_{Dy}}$, $\mathbf{2_{Dy}}$ and $\mathbf{3_{Dy}}$, respectively. Similar subtle changes in the other C_r–C_r (C7-C8 and C9-C10 in $\mathbf{1_{Dy}}$, C1-C2 in $\mathbf{2_{Dy}}$ and $\mathbf{3_{Dy}}$), C–N and C–O bond lengths occur within the indigo ligands of the three complexes, a consequence of which is to enable significant decreases in the intramolecular Dy···Dy distance, which changes from 7.078(1) Å to 6.921(1) Å and to 6.874(1) Å. The shortest intermolecular Dy···Dy distances in the structures of $\mathbf{1_{Dy}}$, $\mathbf{2_{Dy}}$ and $\mathbf{3_{Dy}}$ are 8.978(1), 8.884(1) and 9.089(1) Å, respectively.

Table 1. Selected bond lengths (Å) and angles (°) for $\mathbf{1_{Dy}}$, $\mathbf{2_{Dy}}$ and $\mathbf{3_{Dy}}$.

	$\mathbf{1_{Dy}}$	$\mathbf{2_{Dy}}$	$\mathbf{3_{Dy}}$
Dy–N	2.383(3)/2.391(3)	2.343(4)	2.352(3)
Dy–O	2.246(3)/2.236(3)	2.176(3)	2.217(3)
Dy···Dy	7.078 (1)	6.921(1)	6.874(1)
C_c–C_c	1.391(6)	1.423(4)	1.452(7)
C_r–C_r	1.480(5)/1.481(5)	1.433(6)	1.409(5)
C–N	1.386(5)/1.392(5)	1.398(6)	1.410(5)
C–O	1.257(5)/1.259(5)	1.293(6)	1.334(5)
N-Dy-O	78.4(1)	81.8(1)	83.2(1)
Cp*-Dy-Cp*	138.7(1)/139.4(1)	140.1(1)	137.5(1)
N-C-C-N	177.0(4)	180.0(5)	180.0(4)

Variable-temperature direct current (D.C.) magnetic susceptibility data were collected on all six compounds in the temperature range of 2-300 K. As shown in Fig. 2, the room-temperature $\chi_M T$ values of 15.72 and 28.19 cm^3 K mol^{-1} for $\mathbf{1_{Gd}}$ and $\mathbf{1_{Dy}}$ are in good agreement with the theoretical values of 15.75 and 28.34 cm^3 K mol^{-1} for two uncoupled Gd^{3+} ($^8S_{7/2}$, g = 2) and Dy^{3+} ($^6H_{15/2}$, g = 4/3) ions, respectively. Complexes $\mathbf{1_{Gd}}$ and $\mathbf{1_{Dy}}$ produce similar, slow decreases in $\chi_M T$ down to approximately 10 and 20 K, respectively, and then $\chi_M T$ decreases rapidly to reach minimum values of 10.68 and 10.17 cm^3 K mol^{-1} at 2 K. The observed decrease of $\chi_M T$ for $\mathbf{1_{Ln}}$ can be attributed to a combination of weak antiferromagnetic coupling and/or thermal depopulation of low-lying crystal-field states.

The low-temperature $\chi_M T$ data for $[K(thf)_6][\mathbf{2_{Ln}}]$·thf (Fig. 2), in which the lanthanides are bridged via the radical $[ind]^{3-}$ ligand, contrasts markedly that of $\mathbf{1_{Ln}}$. At 300 K, the $\chi_M T$ values of $\mathbf{2_{Gd}}$ and $\mathbf{2_{Dy}}$ are 15.71 and 28.55 cm^3 K mol^{-1}, respectively, which are slightly lower than the expected values of 16.13 and 28.72 cm^3 K mol^{-1} for two non-interacting Ln^{3+} ions and an S = ½ radical. As the

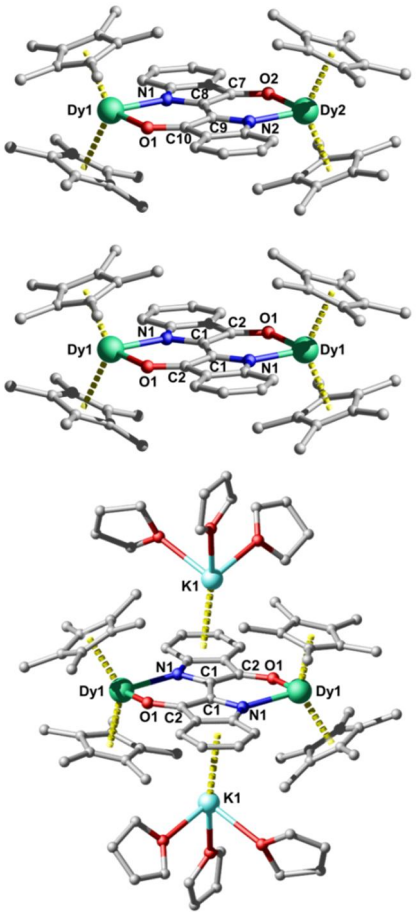

Fig. 1 Structures of $\mathbf{1_{Dy}}$ (top), $\mathbf{2_{Dy}}$ (middle) and $[\{K(thf)_3\}_2(\mathbf{3_{Dy}})]$ (bottom).

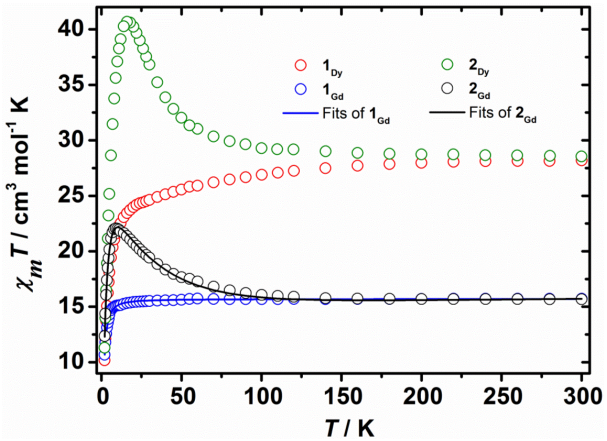

Fig. 2 Plots of $\chi_M T(T)$ for $\mathbf{1_{Ln}}$ and $[K(thf)_6][\mathbf{2_{Ln}}]$ (Ln = Gd, Dy) in an applied field of 10 kOe. The solid lines are fits of the data for Ln = Gd.

temperature decreases, $\chi_M T$ slowly increases down to 50 K, before increasing more rapidly to reach maximum values of 22.07 cm^3 K mol^{-1} at 9 K and 40.68 cm^3 K mol^{-1} at 16 K for **2**$_{Gd}$ and **2**$_{Dy}$, respectively. At lower temperatures, $\chi_M T$ decreases to become 12.34 and 11.30 cm^3 K mol^{-1} at 2 K for in **2**$_{Gd}$ and **2**$_{Dy}$, respectively. The rapid increases in $\chi_M T$ followed by sharp decreases indicate antiferromagnetic magnetic coupling between the lanthanide ions and the radical ligand. The $\chi_M T(T)$ data for [{K(thf)$_3$}$_2$(**3**$_{Ln}$)] (Ln = Gd, Dy) are very similar to those of **1**$_{Ln}$, with values of 15.59 and 28.22 cm^3 K mol^{-1} at 300 K, respectively, and 10.46 cm^3 K mol^{-1} and 10.33 cm^3 K mol^{-1} at 2 K (Fig. S10). The isothermal magnetization (M) vs field (H) plots at 1.8 and 5 K for the six compounds are shown in Figs S11-S16. The curves show rapid increases in the magnetization at low magnetic fields, followed by slow increases in higher fields, reaching saturation values of 14.03 μ_B (**1**$_{Gd}$), 10.39 μ_B (**1**$_{Dy}$), 13.15 μ_B (**2**$_{Gd}$), 10.97 μ_B (**2**$_{Dy}$), 13.78 μ_B (**3**$_{Gd}$) and 11.01 μ_B (**3**$_{Dy}$).

For **1**$_{Gd}$, fitting the $\chi_M T(T)$ and $M(H)$ data using PHI[11] and the spin Hamiltonian $\hat{H} = -2J\hat{S}_{Gd}\cdot\hat{S}_{Gd}$, where $\hat{S}_{Gd}$ is the spin operator for Gd^{3+}, gave an exchange coupling of constant of J = –0.013(1) cm^{-1} and g = 2.00(1), indicating very weak antiferromagnetic interactions between the Gd^{3+} ions, as expected. Using the same model for **3**$_{Gd}$ gave J = –0.018(1) cm^{-1} and g = 1.99(1). For **2**$_{Gd}$, the Hamiltonian $\hat{H} = -2J\hat{S}_{rad}\cdot(\hat{S}_{Gd} + \hat{S}_{Gd})$ produced good fits of the data, with a significantly larger J value of –11.04(16) cm^{-1} and g = 2.01(1). The magnitude of J in **2**$_{Gd}$ indicates that the radical $[ind]^{3-}$ ligand engages in strong direct antiferromagnetic exchange with the Gd^{3+} ions, resulting in an S = 13/2 ground state. Whereas the small exchange coupling constants determined for **1**$_{Gd}$ and **3**$_{Gd}$ are characteristic of gadolinium compounds,[10] the magnitude of the coupling constant in **2**$_{Gd}$ is the second largest determined for a lanthanide complex of a radical ligand. Indeed, the J-value for **2**$_{Gd}$ is exceeded only by that of –27 cm^{-1} (–2J formalism) in [Gd{N(SiMe$_3$)$_2$}(thf)$_2$(μ:η^2:η^2-N$_2$)]–, in which the Gd^{3+} ions are bridged by an $[N_2]^{3-}$ radical.[12]

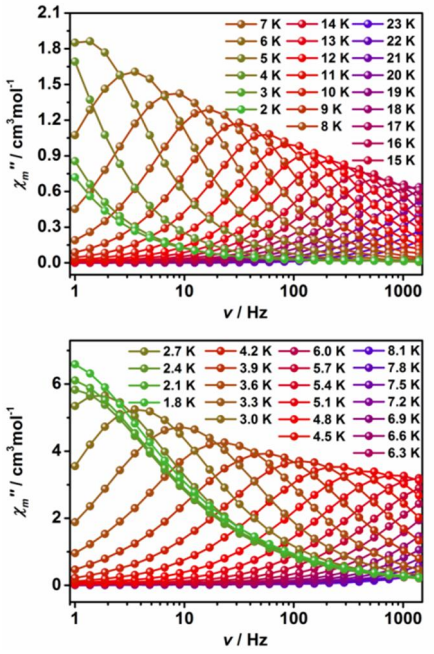

Fig. 3 $\chi''(\nu)$ at various temperatures in zero applied field for **1**$_{Dy}$ (upper) and for **2**$_{Dy}$ (lower).

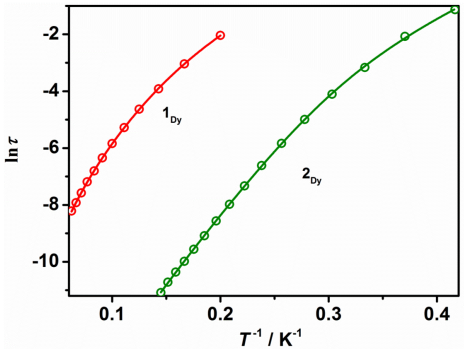

Fig. 4 Temperature dependence of the relaxation time for **1**$_{Dy}$ and **2**$_{Dy}$ (the solid lines are fits of the data).

To probe for SMM properties in the dysprosium-containing compounds, alternating current (A.C.) magnetic susceptibility measurements were carried out. In zero D.C. field, **1**$_{Dy}$ and **2**$_{Dy}$ give rise to frequency-dependent in-phase (χ') and out-of-phase (χ'') susceptibility (Figs 3, S17, S18), confirming their SMM nature. For **1**$_{Dy}$, peaks in $\chi''(\nu)$ were observed in the temperature range 5-18 K. For **2**$_{Dy}$, $\chi''(\nu)$ maxima were observed in a narrower temperature range of 2.7-5.4 K up to the maximum frequency of 1399 Hz. The α parameters were obtained by fitting χ'' vs. χ' Cole-Cole diagrams to a generalized Debye model, which yielded α = 0.02-0.08 for **1**$_{Dy}$ and α = 0.11-0.29 for **2**$_{Dy}$, indicating narrow and moderate distributions of magnetization relaxation times, respectively (Figs S20, S21 and Tables S2, S3). No frequency-dependent signals were observed in the in-phase and out-of-phase susceptibility for **3**$_{Dy}$, hence it is not an SMM (Fig. S19). The A.C. susceptibility data for **1**$_{Dy}$ and **2**$_{Dy}$ were analyzed further by plotting ln τ versus 1/T, where τ is the relaxation time, and fitting the data across the full temperature range using $\tau^{-1} = \tau_0^{-1}e^{-U_{eff}/k_BT} + CT^n$, where τ_0^{-1} and U_{eff} are the Orbach parameters, and C and n are the Raman parameters. For **1**$_{Dy}$, the best fittings gave U_{eff} = 39(1) cm^{-1}, τ_0 = 5.08 × 10^{-5} s, C = 1.72 × 10^{-3} s^{-1} K$^{-5.2}$ and n = 5.2, and for **2**$_{Dy}$ U_{eff} = 35(1) cm^{-1}, τ_0 = 1.60 × 10^{-8} s, C = 2.27 × 10^{-3} s^{-1} K$^{-8.2}$ and n = 8.2 (Fig. 4).

The small anisotropy barriers determined for **1**$_{Dy}$ and **2**$_{Dy}$ can be interpreted in terms of the magnetostructural correlation described above for dysprosium metallocene SMMs.[6] Thus, assuming that the easy axis of magnetization in **1**$_{Dy}$ and **2**$_{Dy}$ is oriented towards the $[Cp^*]^-$ ligands, as has been determined through theoretical studies of many exemplar systems,[6,7] the hard oxygen and nitrogen donors can be regarded as residing in hard (equatorial) plane. As such, the diminished axiality of the Dy^{3+} ion enables efficient relaxation via processes that shortcut the maximum possible thermal energy barrier, hence the low observed U_{eff} values for these systems. The magnetostructural correlation also accounts for the absence of SMM behaviour in **3**$_{Dy}$ since here the formal charge on the ligand is –4, giving rise to particularly strong electrostatic interactions between the indigo ligand and the Dy^{3+} centres in the hard plane.[13] An additional factor that can contribute to the small anisotropy barriers in **1**$_{Dy}$ and **2**$_{Dy}$ (and **3**$_{Dy}$) are dipolar exchange interactions between the Dy^{3+} centres. Such interactions are thought to provide efficient relaxation pathways,[14] and since the intramolecular Dy···Dy distances decrease as the formal charge on the ligand increases, the anisotropy barrier would be expected to diminish, as observed.

The magnetic hysteresis properties of **1**$_{Dy}$ and **2**$_{Dy}$ were studied at 1.8 K using an average field sweep rate of 2.1 mT s^{-1}, which

revealed, in both cases, narrow S-shaped loops that close at zero field and at fields greater than 1.7 T (Figs S22, 23). The closed loop found for the radical-bridged complex $\mathbf{2_{Dy}}$ could be regarded as surprising in light of the ability of some radical ligands to introduce an exchange bias that mitigates the effects of quantum tunneling of the magnetization (QTM), resulting in open hysteresis loops with coercivity.[8] However, additional ligand-based spin alone is insufficient to result in an exchange bias, and factors such as the symmetry of the dysprosium environments and the symmetry relation between them are also important.[15] Since the dysprosium centres in $\mathbf{2_{Dy}}$ engage in strong coupling to the $[ind]^{3-}$ ligand and reside in environments with symmetry that is conducive to SMM behavior, other factors must be involved. The high electrostatic charge on the $[ind]^{3-}$ ligand, especially on the hard oxygen donor atom, and the strength of its interaction with dysprosium, are also likely to play a role in reducing the extent of magnetic blocking.

In summary, the first lanthanide indigo complexes have been described, revealing that the indigo ligand can be accessed in three different oxidation states, i.e. –2, –3 and –4 in $\mathbf{1_{Ln}}$, $\mathbf{2_{Ln}}$ and $\mathbf{3_{Ln}}$, respectively. Through one-electron reduction of $\mathbf{1_{Ln}}$ to give $\mathbf{2_{Ln}}$, strong antiferromagnetic coupling of the lanthanide with the $[ind]^{3-}$ radical can be induced. The exchange coupling constant of J = –11 cm^{-1} describing the interaction between Gd^{3+} and the radical ligand in $\mathbf{2_{Gd}}$ is one of the largest known for a lanthanide. Complexes $\mathbf{1_{Dy}}$ and $\mathbf{2_{Dy}}$ give rise to SMM behaviour in zero D.C. field, however the anisotropy barriers are modest and decrease slightly from 39(1) cm^{-1} in $\mathbf{1_{Dy}}$ to 35(1) cm^{-1} in $\mathbf{2_{Dy}}$, and the hysteresis is hardly affected by the radical nature of the ligand. These observations demonstrate that directly coupled radical ligands in SMMs do not necessarily result in high magnetic blocking temperatures and hysteresis with coercivity, and that factors such as the hard/soft nature of the donor atoms and their formal charge are also important design criteria. Our observations further illustrate the use of organic dyes as ligands in SMMs: previous studies have shown that such systems, e.g. murexide-ligated SMMs,[16] provide a route into correlation of ground state magnetic properties with excited state photophysics, and this aspect will form part of our on-going work.

FSG thanks the EC for a Marie Skłowdowska-Curie International Fellowship (653784). RAL thanks the ERC for the Consolidator Grant 'RadMag' (646740), and the EPSRC for financial support.

Notes and references

1 M. Gsänger, D. Bialas, L. Huang, M. Stolte and F. Würthner, *Adv. Mater*., 2016, **28**, 3615.

2 (a) P. Mondal, M. Chatterjee, A. Paretzki, K. Beyer, W. Kaim and G. K. Lahiri, *Inorg. Chem*., 2016, **55**, 3105. (b) J.-Y. Wu, C.-H.Chang, P. Thanasekaran, C.-C. Tsai, T.-W. Tseng, G.-H. Lee, S.-M. Peng and K.-L. Lu, *Dalton Trans*., 2008, 6110. (c) D. Bhattacharya, C.-H. Chang, Y.-H. Cheng, L.-L. Lai, H.-Y. Lu, C.-Y. Lin and K.-L. Lu, *Chem. Eur. J.* 2012, **18**, 5275. (d) D. V. Konarev, S. S. Khasanov, A. V. Kuzmin, A. F. Shestakov, A. Otsuka, H. Yamochi, G. Saito and R. N. Lyubovskaya, *Dalton Trans*., 2016, **45**, 17095.

3 (a) G. Nawn, K. M. Waldie, S. R. Oakley, B. D. Peters, D. Mandel, B. O. Patrick, R. McDonald and R. G Hicks, *Inorg. Chem*., 2011, **50**, 9826. (b) S. Fortier, J. J. Le Roy, C.-H. Chen, V. Vieru, M. Murugesu, L. F. Chibotaru, D. J. Mindiola and K. G. Caulton, *J. Am. Chem. Soc*., 2013, **135**, 14670.

4 A. Lenz, C. Schmidt, B. Wagner and W. Beck, Z. Naturforsch B, 1997, 52, 474. (b) W. Beck, C. Schmidt, R. Wienold, M. Steimann and B. Wagner, *Angew. Chem. Int. Ed*., 1989, **28**, 1529.

5 (a) D. N. Woodruff, R. E. P. Winpenny and R. A. Layfield, *Chem. Rev*., 2013, **113**, 5110. (b) P. Zhang, L. Zhang and J. Tang, *Dalton Trans*., 2015, **44**, 3923. (c) J. M. Frost, K. L. M. Harriman and M. Murugesu, *Chem. Sci*. 2016, **7**, 2470. (d) J. Liu, Y.-C. Chen, J.-L. Liu, V. Vieru, L. Ungur, J.-H. Jia, L. F. Chibotaru, Y. Lan, W. Wernsdorfer, S. Gao, X.-M. Chen and M.-L. Tong, *J. Am. Chem. Soc*. 2016, **138**, 5441. (e) S. K. Gupta, T. Rajeshkumar, G. Rajaraman and R. Murugavel, *Chem. Sci*. 2016, **7**, 5181. (f) Y.-S. Ding, N. F. Chilton, R. E. P. Winpenny and Y.-Z. Zheng, *Angew. Chem. Int. Ed.*, 2016, **55**, 16071.

6 T. Pugh, N. F. Chilton and R. A. Layfield, *Angew. Chem. Int. Ed*., 2016, **55**, 11082. (b) T. Pugh, F. Tuna, L. Ungur, D. Collison, E. J. L. McInnes, L. F. Chibotaru and R. A. Layfield, *Nat. Commun*., 2015, **6**, 7492. (c) T. Pugh, V. Vieru, L. F. Chibotaru and R. A. Layfield, *Chem. Sci*., 2016, **7**, 2128. (d) T. Pugh, N. F. Chilton and R. A. Layfield, *Chem. Sci*. **2017**, DOI: 10.1039/C6SC04465D.

7 Y.-S. Meng, Y.-Q. Zhang, Z.-M. Wang, B.-W. Wang and S. Gao, *Chem. Eur. J*., 2016, **22**, 12724. (b) S. Demir, J. M. Zadrozne, M. Nippe and J. R. Long, *J. Am. Chem. Soc*., 2012, **134**, 18546. (c) S. Demir, J. M. Zadrozne, and J. R. Long, *Chem. Eur. J*., 2014, **20**, 9524. (d) C. A. Gould L. E. Darago, M. I. Gonzalez, S. Demir and J. R. Long, *Angew. Chem. Int. Ed*., 2017, DOI: 10.1002/anie.201612271.

8 S. Demir, M. Nippe, M. I. Gonzalez and J. R. Long. *Chem. Sci*., 2014, **5**, 4701. (b) S. Demir, I.-R. Jeon, J. R. Long and T. D. Harris, *Coord. Chem. Rev*., 2015, **289-290**, 149.

9 W. J. Evans, C. A. Seibel and J. W. Ziller, *J. Am. Chem. Soc*., 1998, **120**, 6745.

10 See, for example: T. Li, Y. Zhou, X. Li, L. Tian, D. Z. Liao, Z. Y. Liu, J. H. Guo, *RSC Adv*., 2016, **6**, 3058.

11 N. F. Chilton, R. P. Anderson, L. D. Turner, A. Soncini, K. S. Murray, *J. Comput. Chem*., 2013, **34**, 1164.

12 J. D. Rinehart, M. Fang, W. J. Evans and J. R. Long, *Nat. Chem*., 2011, **3**, 538.

13 N. F. Chilton, D. Collison, E. J. L. McInnes and R. E. P. Winpenny, *Nat. Commun*., 2013, **4**, 3551.

14 E. Moreno Pineda, N. F. Chilton, R. Marx, M. Dorfel, D. O. Sells, P. Neugebauer, S.-D. Jiang, D. Collison, J. van Slageren, E. J. L. McInnes and R. E. P. Winpenny, *Nat. Commun*., 2014, **5**, 5243.

15 B. S. Dolinar, S. Gómez-Coca, D. I. Alexandropoulos and K. R. Dunbar, *Chem. Commun*., 2017, DOI: 10.1039/c6cc09824.

16 J. Jung, X. Yi, G. Huang, C. Daiguebonne, O. Guillou, O. Cador, A. Caneschi, T. Roisnel, B. Le Guennic and K. Bernot, *Dalton Trans*., 2015, **44**, 18270.

